CIRCULATION COPY
SUBJECT TO RECALL
IN TWO WEEKS

UCRL-93400
PREPRINT

TANDEM MIRROR TRAPPED PARTICLE INSTABILITY DRIVEN BY AXIAL SHEAR IN E x B ROTATION

J. A. Byers

This paper was prepared for submittal to

The Physics of Fluids

September 6, 1985

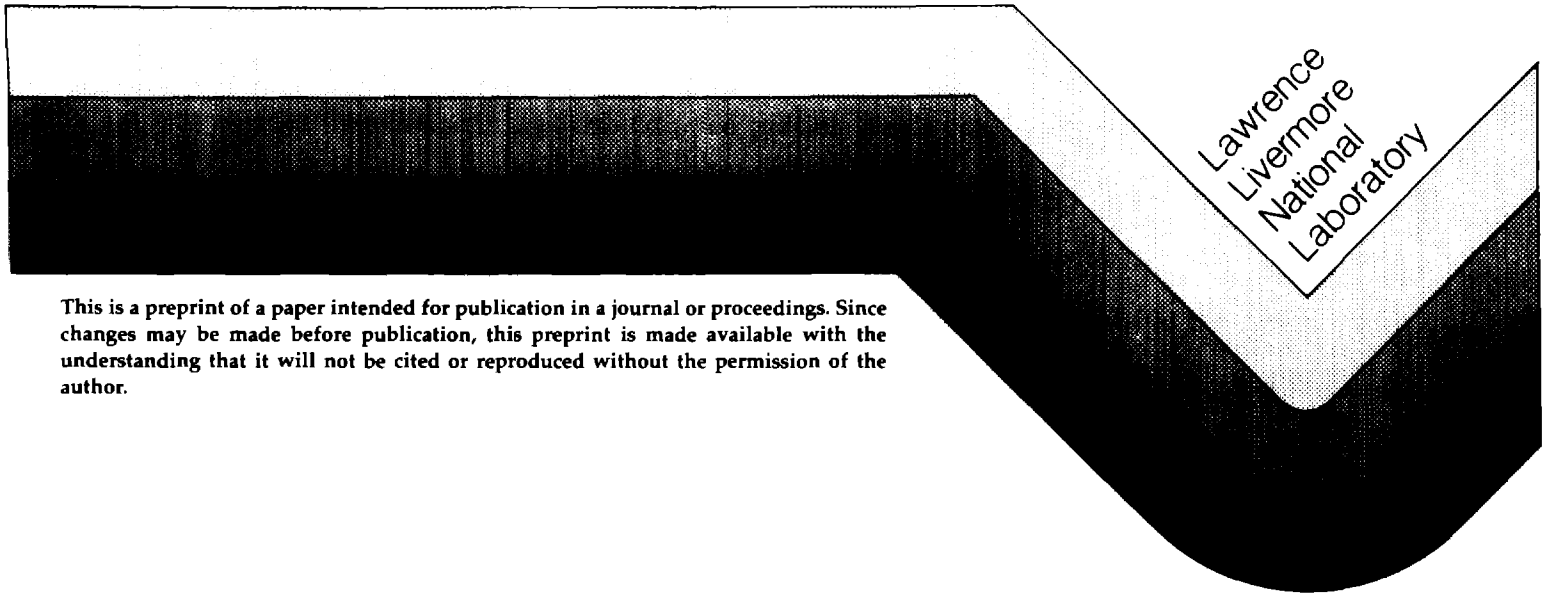

This is a preprint of a paper intended for publication in a journal or proceedings. Since changes may be made before publication, this preprint is made available with the understanding that it will not be cited or reproduced without the permission of the author.

DISCLAIMER

This document was prepared as an account of work sponsored by an agency of the United States Government. Neither the United States Government nor the University of California nor any of their employees, makes any warranty, express or implied, or assumes any legal liability or responsibility for the accuracy, completeness, or usefulness of any information, apparatus, product, or process disclosed, or represents that its use would not infringe privately owned rights. Reference herein to any specific commercial product, process, or service by trade name, trademark, manufacturer, or otherwise, does not necessarily constitute or imply its endorsement, recommendation, or favoring by the United States Government or the University of California. The views and opinions of authors expressed herein do not necessarily state or reflect those of the United States Government or the University of California, and shall not be used for advertising or product endorsement purposes.

Tandem mirror trapped particle instability driven by axial shear in E x B rotation

J. A. Byers

Lawrence Livermore National Laboratory, University of California,

P.O. Box 5511, Livermore, Ca., 94550

We obtain a complete solution for the growth rate and real frequency of electrostatic trapped particle modes driven by the axial shear in the equilibrium $E \times B$ rotational frequency, ω_E, in the eikonal limit for a simplified square well equilibrium model of a tandem mirror. The instability takes on a flute character for some region of parameter space, principally at low mode number and large passing fraction, with a growth rate $\gamma^2 = m^2\overline{(\Delta\omega_E)^2}$, in agreement with prior calculations, but is nonflute elswhere, even with zero curvature. The mode is more unstable for larger passing density in contrast to the curvature driven trapped particle mode which is stable for larger passing density. This feature makes the mode probably more dangerous for more strongly collisional devices. In the flute regime this mode appears identical to the MHD flute version of the shear mode. Depending on the sign of the charge of the passing species and the sign of the change in ω_E, this trapped particle mode can isolate itself to the center cell and thus avoid the stabilizing effect of strong anchor curvature and can do so without paying the MHD penalty for bending the field lines, thus requiring large center cell ion gyro radius for stabilization. For some typical tandem equilibria, this worst form of the mode is not possible since the mode tends to isolate to the anchor rather than to the center cell. In this case the shear in the rotation can also help to stabilize the curvature–driven mode.

I. INTRODUCTION

In the MHD context($E_\parallel = 0$) an instability driven by the axial variation or shear

in the equilibrium $E \times B$ velocity was first discussed by Lee et al,[1] where, in the high Alfven velocity, V_A, limit (flute limit), the growth rate takes the form $\gamma^2 = m^2\overline{(\Delta\omega_E)^2}$, which shows the growth rate increasing linearly with the mode number, m, apparently without limit. This paper did not treat the mode in the context of realistic tandem mirror equilibria with strongly stabilizing curvature in the anchor region. In this case net *flute* stability is presumably given by a net balance of the stable curvature flute frequency with the unstable shear flute growth rate. There is yet no general treatment of ballooning forms of this mode, although for a specialized model ref. 1 describes the mode as axially localized but with large axial wavelength. For a general tandem mirror equilibrium we can expect a localized or ballooning form of this MHD shear mode, where the mode can isolate away from the strong curvature stable regions by paying the penalty for bending the lines of force. This topic is being explored in detail by numerical solution of the time dependent MHD equations by Cohen and Freis.[2]

In the present paper we do not examine the MHD limit($E_{||} = 0$), but instead examine the electrostatic trapped particle limit($A_{||} = 0$). In this limit the mode was first discussed by Berk et al,[3] who found a flute with a growth rate identical to that of the MHD flute form of the the mode. This latter paper also did not discuss how the mode can become nonflute. This is a particularly crucial issue for the usual tandem mirror configuration with strong stabilizing curvature in the anchor region, because electrostatic trapped particle modes are able to isolate to the center cell without paying the MHD penalty of bending field lines. The circumstances under which this can occur for the shear mode are fully discussed for a simple model equilibrium in this paper. We shall see that the physical mechanism for the shear mode is different in the flute and isolated limits. We will also find that the shear mode is more unstable for *larger* passing density in contrast to the curvature-driven mode which is stabilized by larger passing density,[3] and so we are evidently faced with the possibility of some form of a trapped particle mode being unstable for any magnitude of passing density.

In a previously published Letter[4] we derived the basic shear mode dispersion relation and evaluated it for some cases. While the basic results of that Letter are correct(and will be repeated here) the explanation was necessarily terse. This paper expands the discussion and supplies new results, especially concerning the interaction of the shear–driven mode with the curvature–driven mode and the effects of ion finite gyro radius (FLR). This paper also applies the stability criteria derived herein to some simplified models of actual tandem mirror devices. We will find for a variety of two–region tandem equilibria that the shear mode tends to isolate to the anchor and therefore can be stable if the anchor pressure–weighted curvature is large enough.

Using simple square well models for the equilibrium and the usual assumption of electrostatic fields, and the high mode number or eikonal limit of local-in-r modes, we are able to derive and numerically solve the dispersion relation for axial shear driven trapped particle modes. Sec. II describes the equilibrium, sec. III gives a simple description of some aspects of a guiding center drift picture, sec IV describes the solution techniques, sec. V describes the eigenmode solutions for the pure velocity shear mode, secs. VI and VII describe the solutions in the presence of curvature, sec. VIII adds in the effects of finite ion gyro radius, and secs. IX and X sum up the results and draw conclusions.

II. EQUILIBRIUM MODEL

We specialize to two square well regions, modeling a center cell and anchor. We also as the simplest subset of equilibrium models consider the total density and the magnetic field to be constant in z, except for spikes in B at the region boundaries to model the magnetic mirrors. We also take the potential to be constant in z–except for a possible spike at the center cell-anchor boundary– but with a jump in the radial slope at the same boundary, thus giving a jump in the $E \times B$ rotation frequency, $\Delta\omega_E$. That is, our axial equilibrium model is valid only at a single radius where the equilibrium potential has no change in z but where its radial derivative does. We specialize to no passing ions and to

arbitrary passing electron fraction, n_p. In general we will also include curvature drifts of the trapped ions, with different magnitudes and opposite signs in the two regions. This perhaps extremely specialized equilibrium model is useful because it reduces the number of parameters that must be scanned for a complete survey of the instability. For example, with zero curvature, we need only specify the passing fraction, n_p, and δ, the fractional length of the anchor relative to the total half-length. The mode frequencies and growth rates are then determined as a relative fraction of $\Delta\omega_E$, with the absolute value being relatively unimportant. Fig. 1 shows the axial profiles of the various densities and the $E \times B$ drift frequency.

The electron axial equilibrium is assumed to follow the Boltzmann law, which for our model determines the axial variation of $\partial n/\partial r$ through its connection to the axial variation or shear in $\partial\Phi/\partial r$. Collisionless concepts are otherwise assumed even though we scan the solution up to 100% passing density–the rationale being that a collisionless solution for a Boltzmann equilibrium distribution at 100% passing density would be the expected answer for a strongly collisional electron species. And, in fact, our form of the passing electron response for $n_p = 1.$ agrees with that found by Nevins[5] for his strongly collisional solution, as modified for our special equilibrium. Our model will not apply for more intermediate collisionality regimes where more subtle effects can be expected.

The validity of this model for any actual tandem is limited especially considering the variety of possibilities when including both a final potential peak(plug) and a potential depression(thermal barrier) at some intermediate point, and the variety of possible lengths and densities of each region. Accurate answers for realistic tandems probably would require at least a three region model with densities and potentials varying from region to region. Such a model is well within the capabilities of our basic numerical solution technique—more regions will just result in a greater number of roots. At this stage, however, it was deemed more appropriate to stick with the simplest possible equilibrium model in order to exhaustively study the physics of the shear mode instability without the clutter of details

that necessarily accompany a more exact modeling of actual tandem equilibria. We shall see that the mode still has complex behavior, even within the limits set by this perhaps simplest of all possible equilbrium models. Most importantly, the physics of the instability mechanism becomes clearest in such a setting, and should aid our understanding of the results obtained, either numerically or analytically, with more realistic equilibrium models. Moreover, we shall be able to make some limited statements about stability of the simplest of actual tandem configurations, those which can be characterized as dominated by two regions, either with or without a thermal barrier.

It seems useful to display the following definitions of equilibrium quantities. For any function $F(z)$ we define $\overline{F} = (1-\delta)F_C + \delta F_A$, which is the bounce average value seen by the passing electrons or equivalently, for this model, the density weighted average over the entire length.

$$n_p = \text{passing density fraction} \tag{1}$$

$$\delta = \text{fractional anchor length} \tag{2}$$

$$1-\delta = \text{fractional center cell half length} \tag{3}$$

We work in the frame where the passing electrons see zero $E \times B$ drift,

$$\overline{\Delta\omega_E} = \overline{\omega_E} = (1.-\delta)\omega_C + \delta\omega_A = 0 \tag{4}$$

$$\overline{(\Delta\omega_E)^2} = (1-\delta)\omega_C^2 + \delta\omega_A^2 = (\delta-\delta^2)(\Delta\omega_E)^2 \approx \delta(\Delta\omega_E)^2 \tag{5}$$

The density gradient is characterized by the electron diamagnetic drift frequency,

$$\Omega_{*j} = -m/r \cdot (\partial n/\partial r)_j T_e/(neB) = m\rho_s^2/r^2 \left(-\frac{r}{n}\frac{\partial n}{\partial r}\right)_j \omega_{ci} \tag{6}$$

where

$$\rho_s^2 = T_e/(m_i\omega_{ci}^2) \tag{7}$$

Its bounce average value is given by

$$\overline{\Omega_*} = (1.-\delta)\Omega_{*C} + \delta\Omega_{*A} \tag{8}$$

And it can be shown that

$$\overline{\Omega_*} = \Omega_{*C} + m\omega_C = \Omega_{*A} + m\omega_A \tag{9}$$

where the latter equation illustrates the axial variation of the density gradient or of Ω_* and how it is directly related to the axial variation of ω_E. As typical values we usually choose $\Delta\omega_E \approx (10^{-3} \rightarrow 10^{-2})\omega_{ci}$, and a similar range of values for $\overline{\Omega_*}/m$. Note that we are using the convention that $\Omega_j = m\omega_j$, where $_j$ is either $_C$ or $_A$, and where m is the azimuthal mode number. A useful dimensionless expression appearing in the stability analysis is

$$D = n_p(r/m\rho_s)^2 \tag{10}$$

And note that

$$D\Omega_* = \frac{n_p}{m}\left(-\frac{r}{n}\frac{\partial n}{\partial r}\right)\omega_{ci} \tag{11}$$

III. GUIDING CENTER DRIFTS AND CHARGE SEPARATION

Both MHD and electrostatic trapped particle instabilities have simple explanations based on charge separation caused by the effects of the guiding center drift motion. The shear mode should be no exception. The flute limit, while appearing to be the simplest, is actually more subtle in this regard. In the flute limit, there is no difference in the net *average* ion–electron equilibrium $E \times B$ drift, or in the perturbed $\tilde{E} \times B$ drift. With zero curvature and ignoring the rotation(centrifugal) driven drift, then the only guiding center drift remaining that can produce charge separation is the polarization drift, normally thought of as only a reactive response (inertia) of the system to ensure quasineutrality. Here, however, part of the polarization drift, that due to $V \cdot \nabla\tilde{E}$, is responsible for the instability mechanism in the flute limit. Normally, without velocity shear, this drift merely is the necessary drift to account for the doppler shift at the constant rotation frequency. With shear, however, there remains the differential drift between the two regions, and this shows up in the polarization drift, which is, upon averaging over the entire length as is appropriate for a flute mode, for a two region, constant density, equal length model,

$$1/2(\omega - \Omega_C)\phi_C + 1/2(\omega - \Omega_A)\phi_A = 0$$

Now substitute for ϕ_A in terms of ϕ_C using the flute relationship of constant displacement, $\phi_C/(\omega - \Omega_C) = \phi_A/(\omega - \Omega_A)$ and use $\Omega_C = m\Delta\omega_E/2$ and $\Omega_A = -m\Delta\omega_E/2$, to give

$$(\omega - m\frac{\Delta\omega_E}{2})^2 + (\omega + m\frac{\Delta\omega_E}{2})^2 = 0$$

or

$$\omega^2 = -m^2{\Delta\omega_E}^2/4$$

This simple derivation requires that the mode be flute, and other considerations determine when this is valid. In this electrostatic trapped particle model it is clearly the *passing* density that links the two regions, and indeed, in the limit of zero passing density we would have simply two independent regions with independent stable modes doppler shifted at their respective $E \times B$ drift frequencies. Furthermore this supplies the reason that this shear–driven flute mode is more unstable for larger passing fraction, as we shall see, in contrast to the curvature–driven isolated mode that is more unstable for smaller passing fraction. As another comparison, in the MHD ($E_\parallel = 0$) case the shear mode tends to be flute because nonflutes tend to be stabilized by line bending, which effect is completely absent in the electrostatic ($A_\parallel = 0$) case.

In the nonflute limit, when the mode becomes localized strongly to one of the two regions, the guiding center drift explanation is actually simpler: now there is a difference between the equilibrium $E \times B$ drifts of the passing species and its trapped counterpart of oppositely signed charge, since the trapped species sees its local value of the drift (and can no longer be flute averaged with the other trapped species) whereas the passing species sees the drift averaged over the entire length. This differential equilibrium drift acts much like a curvature–driven differential drift. We shall see that this supplies the correct answer for the instability drive in the isolated limit. The rest of this paper gives an explanation of just how the mode makes the transition from flute to nearly isolated, and what stabilizes the mode, and how this shear mode interacts with curvature and FLR.

IV. SOLUTION TECHNIQUE

The technique used in this paper is to write the equations for quasineutrality, assuming electrostatic modes, and assuming bounce averaging of all particle species, in both regions and to then solve the resulting coupled set of equations for the mode complex frequency and the eigenmode relative amplitudes ϕ_C and ϕ_A in the center cell and anchor. When we have zero curvature this results in a cubic dispersion relation, simply because we have only three separate resonant denominators, $\omega - m\omega_C$ for the center cell trapped species, $\omega - m\omega_A$ for the anchor trapped species, and ω for the passing electrons—we work in the frame where the passing electron species sees zero E x B drift. This frame turns out to result in the simplest form of the dispersion relation–any other frame would do as well but at the complication of adding a doppler shift to all of the frequencies. Adding curvature drift to the trapped ions in both center cell and anchor produces an additional two resonant denominators thus resulting in a quintic dispersion relation. Either the cubic or quintic is easily solved with standard root solvers. The results are presented here primarily in the form of graphs of the growth rate and frequency versus some system parameter. It is relatively easy to get a fairly complete map of the solution for this model equilibrium. The parameters scanned are the mode number m and passing density n_p for the pure velocity shear mode. When adding curvature we additionally scan the curvature drift frequencies, principally as the ratio of the curvature-driven-flute frequency relative to $\Delta\omega_E$, and a_i/r, finite ion gyro radius(FLR), principally as a ratio of the ion diamagnetic drift frequency ω_{*i} relative to $\Delta\omega_E$.

During the development of this work, the technique of numerically solving the coupled equations for the eigenmode frequencies was undertaken as a check on the solutions obtained from a linearized bounce average simulation code which is an initial value approach where the real frequency and growth rate of the fastest growing mode are measured from the time dependent solution. Both techniques agree to the limits of measurement accuracy for the simplified square well model described here. The simulation technique is expected

to be more appropriate for nonsquare well models with continuous orbits— limited results have been obtained but will not be discussed in this paper.

V. ELECTROSTATIC MODES IN ZERO CURVATURE LIMIT

In order to elucidate the physics of the velocity shear effect, we first specialize to zero curvature and zero ion gyro radius(the ion inertia or polarization drift is retained). We begin by writing the equations of quasineutrality in the high mode number m limit, assuming local-in-r solutions, using the electrostatic limit ($A_{\|} = 0$), and bounce averaging the response for all species. As discussed in the section on equilibrium we have restricted our model to five different species, center cell trapped ions and electrons, anchor trapped ions and electrons, and passing electrons. Later we will allow our ion species to experience curvature drifts, but here we will start with only the $E \times B$ drift frequency with a jump in its value, $\Delta\omega_E$, at the center cell- anchor boundary, with values ω_C in the center cell and ω_A in the anchor. We write each of the charge separation terms in terms of the perturbation potentials in the center cell and anchor, ϕ_C and ϕ_A. This results in two coupled equations which must then be solved for the (complex) value of the eigenmode frequency, ω. In the center cell we have

$$-\phi_C - D\delta(\phi_C - \phi_A) + \frac{D\Omega_{*C}\phi_C}{\omega - \Omega_C} - \frac{D\overline{\Omega_*}((1.-\delta)\phi_C + \delta\phi_A)}{\omega} \tag{12}$$

and in the anchor we have

$$-\phi_A - D(1.-\delta)(\phi_A - \phi_C) + \frac{D\Omega_{*A}\phi_A}{\omega - \Omega_A} - \frac{D\overline{\Omega_*}((1.-\delta)\phi_C + \delta\phi_A)}{\omega} \tag{13}$$

The terms in Eq. (12) and Eq. (13) are respectively, the polarization drift of the trapped ions, the Debye shielding from the passing electrons, the trapped ion minus the trapped electron $E \times B$ drift, and the passing electron $E \times B$ drift. We have divided through by the coefficient of the polarization term, $(m^2/r^2)(\omega_{pi}^2/\omega_{ci}^2)$. These equations differ from the zero shear limit only in the axial variation of ω_E in the different resonant denominators, and as reflected in the axial variation of Ω_*. Note in particular the last term in these equations,

that for the passing electron $E \times B$ response which is seen to be proportional to the *bounce average* value of Ω_*. This result is a natural consequence of the bounce average formalism as applied to the guiding center drift equations. In the high bounce frequency limit the average radial drift motion is proportional to the bounce average of the wave potential, $\overline{\phi}$. But now, in the presence of an axial variation in ω_E and in Ω_* the novel feature is that this average radial motion encounters an equilibrium radial density gradient that is also a function of the orbit path in z, with the result that the average charge separation, which is distributed uniformly over the entire orbit, must be calculated using the bounce average of the density gradient or of Ω_*. This result also has been independently derived, starting from the drift kinetic equation, by R. H. Cohen.[4]

Eqs. (12),(13) can be manipulated to give the following symmetric form:

$$\phi_C \left[\omega(\omega - \Omega_C) + D\delta(\omega - \overline{\Omega_*})(\omega - \Omega_A)\right] - \phi_A D\delta(\omega - \overline{\Omega_*})(\omega - \Omega_C) = 0 \qquad (14)$$

$$\phi_A \left[\omega(\omega - \Omega_A) + D\delta(\omega - \overline{\Omega_*})(\omega - \Omega_C)\right] - \phi_C D\delta(\omega - \overline{\Omega_*})(\omega - \Omega_A) = 0 \qquad (15)$$

In this limit of zero curvature there were only three distinct resonant denominators, ω, $(\omega - \Omega_C)$, and $(\omega - \Omega_A)$, and the net result upon eliminating ϕ_C, ϕ_A is a cubic dispersion relation for the eigenmode frequency ω, which can be put in the form

$$\omega(\omega - \Omega_C)(\omega - \Omega_A) + D(\omega - \overline{\Omega_*})\left[\delta(\omega - \Omega_A)^2 + (1. - \delta)(\omega - \Omega_C)^2\right] = 0 \qquad (16)$$

From this equation we can immediately see one important limit, $D \rightarrow \infty$, where the equation reduces to the product of a single real root, $\omega = \overline{\Omega}_*$, and a quadratic, with the resulting dispersion relation,

$$\omega^2 = -m^2\overline{(\Delta\omega_E)^2} \qquad (17)$$

and from either Eq. (14) or Eq. (15) it can be seen that the eigenmode satisfies the *flute* form,

$$\phi_C/(\omega - \Omega_C) = \phi_A/(\omega - \Omega_A) \qquad (18)$$

which states that the plasma displacement is constant, $\xi_C = \xi_A$. This flute limit with growth rate $\gamma^2 = m^2\overline{(\Delta\omega_E)^2}$ is identical to that obtained in the MHD flute limit by Lee et al,[1] and agrees with the electrostatic trapped particle mode answer obtained by Berk et al,[3] where these latter two have been evaluated in the zero ion gyro radius limit. So we have the first result, that the trapped particle shear mode is identical to the MHD shear mode in the flute limit. This limit may be the least interesting, however, as we anticipate that the trapped particle mode can more easily localize to avoid strong stabilizing regions—this point will be examined in detail further on when we include curvature drifts.

If we substitute the flute form of the mode into Eqs. (12) and (13) we get all terms cancelling out except the first, that due to the polarization drift, which confirms our earlier analysis.

Before proceeding to the numerical solution of the full cubic dispersion relation, let us see if we can obtain more useful information by making certain assumptions. The most obvious limit is to assume that the mode can completely localize to one or the other of the two regions (even in this zero curvature limit). This assumption will later be justified and its range of validity determined by the full numerical solution. To look in this limit we need merely set $\phi_A = 0$ in Eq. (12). When we do this we obtain another quadratic

$$-\omega^2 + \omega m\omega_C + n_p\omega_C\omega_{ci}\left(-\frac{r}{n}\frac{\partial n}{\partial r}\right) \approx 0 \tag{19}$$

where we here have taken the limit $D << 1$, since we have already seen that the opposite limit $D >> 1$ is the flute regime. This fully isolated limit, Eq. (19), predicts an instability drive that is proportional to $n_p\omega_C$ and a stabilizing term $\omega m\omega_C$, similar to the physics of a fast drift term. The usual overshoot stabilizing term (due to the different bounce average of the wave potential $\overline{\phi}$ experienced by the passing electrons and the trapped ions) also proportional to ω, is ignored here since this fully isolated limit turns out to be valid only in the high mode number regime where this term is small since it scales as $1/m$. Marginal stability is approximately given by the following relation between mode number, m, and

passing fraction, n_p,

$$m^2\omega_C/4 \gtrsim n_p\omega_{ci}\left(-\frac{r}{n}\frac{\partial n}{\partial r}\right) \tag{20}$$

and we see that this limit predicts a lower bound on n_p for instability, i.e., this shear mode is more unstable for *larger* passing fraction, in contrast to the result for the curvature driven trapped particle mode. Moreover, the physical mechanism for instability in this nonflute regime can be seen to be the *differential equilibrium* $E \times B$ drift between the fractional density n_p of trapped ions and the passing electrons. That is, the trapped ions experience a nonzero $E \times B$ drift whereas the passing electrons see zero drift, and we know this to be the usual mechanism for interchange instability where in the present case the differential $E \times B$ drift takes the place of the conventional curvature drift. In this picture stability is dictated by the sign of the differential ion- electron drift and so we can immediately predict that the region to which the nonflute form of the mode will tend to isolate is that with the negative sign of ω_E—remember we are in the frame where the passing electrons see zero $E \times B$ drift.

From this fully isolated approximation, Eq. (19), we can also obtain an approximate answer for the maximum shear driven growth rate:

$$\max \gamma_s^2 \approx n_p\Delta\omega_E\delta\,\omega_{ci}\left(-\frac{r}{n}\frac{\partial n}{\partial r}\right) \tag{21}$$

These features of the fully isolated approximation are in fact confirmed by the full solution of Eq. (16)—but only when the mode is not 'near' the flute regime. In the flute regime, the physical explanation is not as intuitive and it is certainly *not* the differential drift, because the flute average of the differential $E \times B$ drift is identically zero. The flute limit, which is also identical to the flute limit in the MHD version, can only be explained by an effect of the $E \times B$ shear on the ion polarization drifts, or said another way on the ion inertia. In any case the numerical solution of Eq. (16) shows a smooth transition from the flute regime to the nonflute. Fig. 2 shows a plot of the growth rate and frequency vs mode number, m. The growth rate is seen to equal the flute value, in agreement with

Eq. (17), $\gamma \propto m$, at low mode number, then to peak and finally to drop to zero at some large m. In the low mode number regime, the real frequency is zero, also in agreement with Eq. (17), and also in Fig. 2, a plot of the displacement ratio ξ_C/ξ_A shows this ratio to equal unity here, further substantiating the description of the mode as a flute in this regime. Away from this low mode number, flute regime we find that the mode tends to isolate more and more to the region with the negative ω_E, just as was predicted from our fully isolated approximation. Also, the marginal stability m value is given reasonably accurately by that approximation, Eq. (20). In particular, the scaling of the marginal n_p with m^2 is clearly seen in Fig. 2. So in general we see a strong dependence of the growth rate on the passing density, unlike the flute limit which has no dependence at all— rather, the flute regime growth rate is independent of n_p, but the region of validity of the flute limit shrinks as the passing fraction, n_p, falls.

The flute result and the isolated marginal m, Eq. (20), illustrate another limit occasionally used as an aid to simplifying the results in a more general analysis, the limit where the center cell is extremely long, or the anchor extremely short, $\delta \to 0$. We see that the marginal m, and therefore also the range of m where the mode is flute, goes inversely with δ and that the flute growth rate is proportional to $\delta^{1/2}$. So in this limit the analytic prediction would be that the mode was *always* flute. We can now see that this result is a consequence of taking the long center cell limit and not an absolute characteristic of the mode itself.

VI. EFFECT OF CURVATURE ON THE SHEAR–DRIVEN MODE

When we add in curvature drifts for the trapped ion species, our dispersion relation is modified from the previous cubic to a quintic, less easily approximated, but still easily solved numerically. In broad terms, we can expect the solutions to be affected in two distinct ways. One, the curvature drifts drive the usual trapped particle mode, as described in ref. 3, and in the next section we discuss how velocity shear affects this mode. Two,

curvature can be expected to modify the solutions of the shear-driven mode and this topic is what we now develop. Net *flute* stability, perhaps the most obvious issue, can be expected to be determined simply by algebraically adding the curvature flute drive(stable) to the velocity shear flute drive(unstable). The more interesting possibility arises, however, when the condition for net flute stability is satisfied, and where the passing fraction is much larger than the minimum needed to stabilize the curvature driven trapped particle mode, but where the mode can still go unstable to the velocity shear mechanism by isolating away from the strongly stable curvature region. From our previous discussion about how the mode likes to isolate to the region with negative ω_E, we anticipate that in the presence of strongly stable curvature in the anchor, the mode can isolate to the center cell only if this is the region with negative ω_E.

These concepts are generally confirmed by the numerical solution, as shown in Fig. 3. We see that for the positive ω_C case, sufficiently strong anchor curvature can stabilize the mode, but for the negative ω_C case, we still have a region of instability, and this mode is localized to the center cell. It seems worthwhile to examine in detail the results shown in Fig. 3. For the positive ω_C case complete stability occurs once the flute stability condition is satisfied, i.e., when the flute curvature stability drive equals or exceeds the flute shear instability drive. More specifically this is given by $\omega_{fc} \geq \max \gamma_s$, where ω_{fc} is the curvature driven flute frequency, and where γ_s is the shear driven growth rate. For the zero curvature case we had the maximum $\gamma_s \approx 4.2\Delta\omega_E$. And we now see that complete stability occurs when $\omega_{fc} \approx 4.5\Delta\omega_E$, which is very good agreement. Before becoming completely stabilized this positive ω_C case is characterized by a mode with displacements $\xi_A > \xi_C$, although when the curvature is relatively strong the ratio of the two displacements is of order unity, which is sensible since we would not expect an unstable mode to localize entirely to the anchor which has the strong stabilizing curvature, unlike the zero curvature case where the positive ω_C shear mode does localize to the anchor at high m.

Now compare the foregoing to the detailed mode behavior for the negative ω_C case.

Here we have instability for a range of mode numbers regardless of the strength of the anchor curvature. The unstable mode is characterized by $\xi_C > \xi_A$ and now the mode can again isolate almost completely to the center cell, for the higher mode numbers. Indeed, the growth curve for the higher mode numbers shows very little difference from the zero curvature case. The ability of the mode to isolate almost completely to the center cell may be its most worrisome feature, and the one that makes it presumably more dangerous than the MHD version which would have to pay the line bending penalty in order to isolate away from the anchor.

These results produce the following simple scalings for the shear mode and how it is affected by the flute average of the curvature. Stabilization of the shear mode in its flute or near-flute form by curvature requires $\omega_{fc}^2 \geq m^2\overline{(\Delta\omega_E)^2}$, which the numerical results confirm to be a precise condition for low m. An approximate condition for complete stability to flute modes can be stated as $\omega_{fc}^2 \gtrsim \max \gamma_s^2$, or $\delta\, \omega_{kA}\omega_{ci} \gtrsim \delta\, n_p \Delta\omega_E \omega_{ci}$, which gives $\omega_{kA} \gtrsim n_p \Delta\omega_E$, where ω_{kA} is the mean curvature drift frequency in the anchor. We will not attempt to evaluate this criterion for real devices, except to note that it does appear possible for some conditions, particularly for the lower values of n_p. When it is satisfied the positive ω_C case is completely stable against the shear mode, even for zero FLR. The negative ω_C case is also stabilized in its flute form, but this still allows an unstable shear mode isolated to the center cell at low and moderate mode number. Complete stability in this latter case would require sufficient FLR in the center cell.

To the extent that strong anchor curvature will force the mode to completely isolate to the center cell, we can analyze the stability condition from just our original center cell equation (which had zero curvature), Eq. (12), by taking the limit $\phi_A \rightarrow 0$. This is similar to our previous completely isolated approximation, but now we are invoking other reasons for the isolation and we want to examine the nature of the stability condition at low mode number where usually $D >> 1$. Putting $\phi_A = 0$ in Eq. (12) gives

$$(\omega^2 - \omega\Omega_C)(-1 - D\delta) + \omega D(\overline{\Omega_*} - \Omega_C) - (\omega - \Omega_C)D\overline{\Omega_*}(1 - \delta) = 0 \qquad (22)$$

Collecting terms of like powers of ω gives

$$\omega^2(-1 - D\delta) + \omega\left[\Omega_C(1 + D\delta) - D\Omega_C + D\delta\overline{\Omega_*}\right] + \Omega_C D\overline{\Omega_*}(1 - \delta) = 0 \qquad (23)$$

The expression linear in ω has three distinct terms. The last is the usual overshoot term,[3] the middle term is an additional overshoot term induced by the shear, which will add to the usual overshoot term in our negative Ω_C case, and the first is a shear-induced fast drift term, which will be opposite in sign to the overshoot terms, but smaller by a factor δ. (In contrast, in the high m limit we have previously seen that the fast drift term dominates over the overshoot terms). Analysis of this equation (which has zero FLR) in the large D or low m limit indicates that instability is possible, and the results approximately agree with those obtained from a numerical solution of the full quintic dispersion relation. Both cases shown in Fig. 3 used the $n_p = 1.0$ limit, where the lower mode numbers are stable, indicating that not only is the mode flute stabilized by the curvature, but that the localized form of the mode is also stabilized by the overshoot terms, in this low m regime. Results for lower values of n_p are similar as regards the high m regime, with the maximum unstable mode number scaling as $\sqrt{n_p}$, as was already seen in Fig. 2. However, the lower n_p values, say $n_p \approx 0.1$, now generally show the region of instability extending down to the very lowest mode numbers, $m = 1, 2$, evidently because the overshoot stabilizing terms are less effective at lower passing fraction. These low m unstable modes are of the most concern, since it will be more difficult to stabilize them with FLR. A typical $n_p = 0.1$ result is discussed in sec. VIII.

For the positive ω_C case there is the possibility of *increased* stability over a limited parameter range. (remember that the curvature drifts alone can drive the trapped particle mode if the passing density is too low.) Here, for positive ω_C where the velocity shear tends to drive instabilty only in the anchor which is strongly stabilized by the anchor curvature, and to add to stability in the center cell where the curvature is driving it unstable, we

can have the range of stable passing density extended to lower values as compared to the zero shear case. This has in fact been observed in our model and is discussed in more detail in the next section. The point of bringing up this issue here is to contrast its effect of the possibility of net greater stability(relative to the zero shear case) to the effect of primary interest in this section which was the possibility of greater instability(relative to the zero shear case) for the negative ω_C. The tendency for and physical explanation of either possibility is unambiguous for the present model and should guide the interpretation of solutions in more realistic equilibria.

VII. EFFECT OF SHEAR ON THE CURVATURE–DRIVEN MODE

There are other issues requiring explanation when we consider the simultaneous presence of both shear and curvature. Clearly, if the shear is very weak in some sense then we should obtain nearly just the standard curvature-driven trapped particle mode as discussed in ref. 3. And, if the curvature is very weak in some sense then we should obtain nearly just the simple shear mode as described in sec. V. So we first need to determine what is meant by weak and over what parameter range either of these single effect regimes could be expected. More generally, whereas the previous section dealt with the effect of curvature on the shear mode, this section treats the converse, the effect of shear on the curvature-driven trapped particle mode, and attempts to determine the conditions for which both modes are simultaneously present. Since net stability regardless of the drive is the real issue, we need to be aware of the curvature driven mode and to see if it can be described as a separate mode or as somehow combined with the shear mode, which itself we have already seen to be modified by the flute average effect of the curvature. In the examples of the previous section, we chose conditions such that the curvature mode did not appear for the low mode numbers of interest, $m \lesssim 50$.

First determine the condition for the curvature-driven flute frequency to equal or exceed the maximum shear-driven growth rate. This is expressed as $\omega_{fc} \geq \max \gamma_s$, or as

$\alpha\gamma_c \geq (n_p \Delta\omega_E \delta\omega_{ci})^{1/2}$, where α is the ratio of the curvature-driven flute frequency to the curvature-driven center cell growth rate. As typical values, for $\Delta\omega_E, \gamma_c$ both $= 10^{-2}\omega_{ci}$, this gives $\alpha \geq 5$, which agrees well with our observed value of 4.5 in Fig 3. For $10^{-2} \rightarrow 10^{-3}$, this gives $\alpha \geq 15$. When α is significantly less than these values, the system can be considered to be dominated by the shear mode, since even on a flute average basis the curvature is weak. On the other hand when α satisfies the above criterion, it still may be that the shear mode can dominate, by its ability to isolate to the center cell. As a condition to determine domination by the curvature mode we might simply take $\gamma_c \geq \max \gamma_s$.

We observe a pronounced effect on the curvature mode when there is sufficiently strong shear. In the regime where $\Delta\omega_E \sim \gamma_c$ the curvature mode starts at a marginal mode number that is a factor $1./\delta = 4.0$ times as high as the zero shear limit. This result appears connected to the fact that in this limit the mode takes on a real frequency nearly equal to $m\omega_C$, which makes sense if the curvature mode is indeed highly isolated to the center cell. Assuming first that the mode isolates to the center cell reduces the general quintic dispersion relation to a cubic:

$$-\phi_C - D\delta\phi_C + \frac{D}{n_p}\Omega_{*C}\left(\frac{1}{\omega - \Omega_C - \Omega_K} - \frac{1-n_p}{\omega - \Omega_C}\right)\phi_C - \frac{D\overline{\Omega_*}(1-\delta)\phi_C}{\omega} = 0 \qquad (24)$$

where Ω_K is the curvature drift frequency in the center cell. Rationalizing the denominators gives

$$\omega(\omega-\Omega_C)^2(-1-D\delta)+\omega(\omega-\Omega_C)D\Omega_{*C}+\omega\Omega_K(1-n_p)\omega_{ci}/m-(\omega-\Omega_C)^2D\overline{\Omega_*}(1-\delta)=0 \qquad (25)$$

Then, making the further assumption that $\omega \approx m\omega_C >> \gamma_c$ reduces the cubic to a quadratic in the doppler shifted frequency $\omega - m\omega_C$ since the last term can be dropped compared to the second, and then the constant ω factor cancels out. In this form the fast drift part of the term linear in frequency seen in Eq. (19) has disappeared and we have only what appears to be the usual overshoot[3] term but with the factor δ replaced by unity. This occurs because in this high frequency regime, the trapped ion response dominates

completely the passing electron response rather than just being a factor δ larger as in the zero shear limit. This is simply due to the different resonant denominators, for ions being $\approx \omega - m\omega_C \approx i\gamma_c$ and for the passing electrons being $\omega \approx m\omega_C$. So this analysis would say this limit would pertain so long as $m\omega_C >> \gamma_c$, and failure of this criterion should in some sense define what is meant by weak shear so that a nearly unchanged curvature mode occurs. This criterion is similar to our previously suggested rule for the weak curvature limit. When $\Delta\omega_E = \gamma_c$ this reduces to $m\delta \geq 1.0$, so here this condition would not hold at the lowest mode numbers of interest, but other conditions can easily be imagined where it would hold even at $m = 1$. To summarize, sufficiently strong $E \times B$ shear increases the stability of the curvature driven trapped particle mode by multiplying the overshoot term by a factor $1/\delta$, which therefore allows marginal stability for a higher mode number or a lower passing fraction.

The marginal instability condition for the curvature driven mode due to the shear-modified overshoot in the small D limit is $n_p/(2m) \leq \gamma_c/\omega_{ci}$. As specific examples, for n_p approaching unity instability requires $m > 50$ for $\gamma_c/\omega_{ci} = 10^{-2}$, and $m > 500$ for $\gamma_c/\omega_{ci} = 10^{-3}$, where both of these mode number limits will normally be completely stabilized by even very weak FLR. In contrast, for $n_p \approx 0.1$, instability will occur for mode numbers a factor of 10 smaller than these, so that, while the $\gamma_c/\omega_{ci} = 10^{-3}$ case will stabilize with weak FLR, for the $\gamma_c/\omega_{ci} = 10^{-2}$ case, the marginal m is now as low as 5 and so this curvature mode is in the low or moderate m range and must be considered along with the shear mode(itself modified by flute average of the curvature).

The curvature driven mode is sometimes clearly identified as completely separate from the shear driven mode, especially when it is well separated in mode number–in this limit the curvature mode is mainly at high m where even small FLR will completely stabilize it, leaving only shear driven mode at low or moderate m. Even when the mode number range overlaps, the two modes can be really distinct, as for example when the shear mode is dominated by its anchor region amplitude for the positive ω_C case, and the curvature

mode isolates nearly completely to the center cell. And, plots of γ vs m for this case(not shown here) show two intersecting but distinct curves. But, for the opposite, negative ω_C case with the shear mode itself dominated by its center cell amplitude, then the two modes appear to interact, since here the γ vs m plots show a single merged curve(not shown here).

VIII. FINITE ION GYRO RADIUS

In this section we add in the effects of finite ion gyro radius. First examine the zero curvature limit, the pure velocity shear mode of sec. V. In the discussion of the velocity shear mode in ref 4., the authors gave an approximate rule for stabilization by finite ion orbit effects, $\omega_{*i} \gtrsim \langle \Delta\omega_E \rangle$. Their rule is based on the flute approximation, however, where the mode with zero a_i/r has a growth rate increasing with m, apparently without limit. This same rule comes out automatically from our flute limit, Eq. (17), if we add to the left hand side the usual FLR term, $-\omega m \omega_{*i}$. We see that the answer is naturally cast in terms of the root-mean-squared value, $\langle \Delta\omega_E \rangle$. It is this flute limit rule that predicts no FLR stabilization simply by increasing the mode number, but instead requires sufficiently large a_i/r to stabilize even the low m. And, numerical solutions confirm that the entire low m range is nearly simultaneously stabilized at the same value, $\omega_{*i} \gtrsim \langle \Delta\omega_E \rangle$, which we will call the 'flute limit' value.

But now we have seen our more complete solution with a growth rate peaking out and then dropping to zero as we increase the mode number m, and so we expect that imposing weak finite ion gyro radius will selectively first stabilize or modify the high mode numbers. More quantitatively, the high m stability characteristics are determined by the addition of FLR to our fully isolated approximation, Eq. (19), where we now see that the fast drift stabilization and FLR stabilization terms are of the same sign, for the case of interest, negative ω_C. Thus the two stabilization effects will add, and the addition of weak FLR will first decrease the maximum unstable mode number, and then abruptly stabilize the entire range when $\omega_{*i} \gtrsim \langle \Delta\omega_E \rangle$, determined by the flute limit. If the passing species were

of opposite sign of charge, ions instead of electrons, this model predicts first an *increase* in the maximum unstable mode number as weak FLR is added, since then the FLR and fast drift terms subtract. But the final complete stabilization criterion is still accurately given by the flute limit.

In the presence of curvature as in section VI the results can be expected to be more complex since the zero gyro radius limit itself has a complex stability behavavior as a function of mode number. In particular, we have seen that the shear-driven mode now can possibly isolate to the center cell at low mode number, where the most effective stabilization mechanism is not the fast drift term but the overshoot term (as modified by the shear). With the addition of FLR, determination of net stability requires careful attention to the relative signs of the two principal stabilization terms, overshoot and FLR. In the isolated limit, evaluation of stability would then follow a balancing of terms similar to that required for the curvature driven trapped particle mode,[3] which, for passing electrons exhibits opposite signs for the FLR and overshoot terms, and also exhibits an increased inertia coefficient caused by the Debye shielding that supresses the effectiveness of the FLR term at the lowest mode numbers. All of these features can be seen in our isolated approximation, Eq. (19) if we add in the proper FLR term, $-\omega m\omega_{*i}$. (But remember that Eq. (19) has only the shear drive, i.e., no curvature.) For complete stabilization the FLR amplitude must exceed twice the overshoot term, much larger than the flute limit, since FLR now subtracts from the overshoot stabilization.

For detailed results, let us first examine the rather special limit of 100% passing fraction, $n_p = 1$, where the shear mode as modified by curvature is *not* unstable for the low mode numbers. Results are shown in Fig. 4. Part (a) shows the positive ω_C case, when anchor curvature is chosen to be insufficiently strong to supply complete stability ($\omega_{fc} \approx 11\Delta\omega_E$, and $\max\gamma_s \approx 14\Delta\omega_E$). Here we see a changing window-in-mode-number region of instability, with instability persisting for even the very large a_i/r. This latter behavior is similar to that predicted for the curvature driven trapped particle mode,[3]

where finite ion gyro radius stabilization is of opposite sign to the stabilization provided by the overshoot of a passing electron species—at some m value the two effects cancel and instability reappears. Evidently, a similar competition of stabilizing effects is occuring here. Now however we have three competing stabilizing terms, FLR, overshoot, and fast drift, although this last one is usually only important at the highest mode numbers. For passing electrons, FLR and overshoot have opposite signs, and FLR and fast drift have the same sign. The sign of both the overshoot and fast drift change with the sign of the charge of the passing species, so that if the passing species were ions instead of electrons this window of instability at high a_i/r would not be present.

Fig 4(b) shows the negative ω_C case, where we have chosen the anchor curvature strong enough to provide flute stability ($\omega_{fc} \approx 20\Delta\omega_E$, and $\max\gamma_s \approx 14\Delta\omega_E$), but where instability persists in a middle range of mode numbers. Here, increasing a_i/r stabilizes first the high mode numbers and finally the entire range. Complete stability is reached for this example when $a_i/r \gtrsim 0.03$, or when $\omega_{*i} \gtrsim \Delta\omega_E$, very nearly the same as the zero curvature flute limit. No window of instability is observed here at higher values of a_i/r, apparently because the stronger curvature flute stabililty prevents the mode from isolating at low m and thus prevents overshoot from becoming significantly large.

Now examine the lower passing fraction case, $n_p = 0.1$, for negative ω_C, in Fig. 5, where we can see that the unstable mode numbers extend down to $m = 1, 2$. That is, the lower passing fraction lowers the instability drive but also reduces the effectiveness of the overshoot causing even the lowest mode numbers to be unstable, in contrast to the $n_p = 1.0$ case where the low mode numbers were stabilized by the overshoot. Now, when adding FLR, instability at low m will at first be increased, due to the opposite sign of the FLR and overshoot terms for the passing electron case. Stability can occur only when FLR is sufficiently strong to make up for this cancellation. Compared to $n_p = 1.0$, where we had stability at all m for $a_i/r \gtrsim 0.03$ or $\omega_{*i} \gtrsim \Delta\omega_E$, now with $n_p = 0.1$, stability at all m (with the last one unstable now being $m = 1$) requires $a_i/r \gtrsim 0.3$ or $\omega_{*i} \gtrsim 100\Delta\omega_E$, or

stability for say $m = 3$ requires $a_i/r \gtrsim 0.11$ or $\omega_{*i} \gtrsim 10\Delta\omega_E$. In contrast, for the opposite sign of charge of passing species, the FLR need only slightly enhance the overshoot term, and we find again very nearly that the flute limit pertains, i.e., $\omega_{*i} \gtrsim \Delta\omega_E$, even for $m = 1, 2$. While our results for the low m can not be quantitatively correct, the general scaling should be valid, and it is worth emphasizing again that it is these isolated modes at low mode number that are the most dangerous, particularly for the passing electron case, since the low mode numbers have the FLR term most severely depressed by the enhanced inertia term. And, because this negative ω_C mode tends to isolate to the center cell, this finite gyro radius stabilization is primarily a property of the center cell parameters, i.e., large a_i/r in the anchor will be of little help.

As a final point, note that for Fig. 4 we have chosen $\Delta\omega_E = 0.001\omega_{ci}$, whereas for Fig. 3 we had $\Delta\omega_E = 0.01\omega_{ci}$. This difference is the cause of the different range of unstable mode numbers in Figs. 3 and 4, and is explained fully by our completely isolated approximation, Eq. (20), which shows that the maximum unstable mode number is *inversely* proportional to $(\Delta\omega_E)^{1/2}$.

IX. PHYSICS SUMMARY

A final summary when all effects, shear, curvature, and FLR are included: Distinguish between the curvature driven mode and the shear driven mode, and also distinguish between net flute stable and unstable. First, when the anchor curvature is strong enough to supply net flute stability, then only the negative ω_C case is unstable to the shear mode. This case, in the limit $n_p = 1.0$, is stable for the low mode numbers but unstable at moderate m by localizing to the center cell. For lower, more realistic, values of passing fraction, say $n_p \approx 0.1$, the mode is unstable even for the lowest mode numbers, $m = 1, 2$, and it is this latter regime that requires quite large center cell FLR to obtain stability, if the passing species is electrons. Second, when the anchor curvature is not strong enough to supply flute stability then either sign of ω_C is unstable to the shear mode for some range

of mode numbers, and with FLR included we now have the possibility of a window-in-m remaining unstable even for large a_i/r. Generally, larger passing fraction makes the shear mode more unstable, although when the mode isolates to the center cell there can be subtle tradeoffs creating a situation for the lowest mode numbers where the system can go towards stability by increasing the passing fraction. Finally, the curvature driven mode can have its stability improved by the shear increasing the overshoot stabilization. (And a cautionary note: the very low mode numbers, especially m = 1, will require corrections to any results obtained in this paper—see the discussion further on in sec. X.)

We are now in a position to draw some limited conclusions about stability of this shear mode in simplified actual tandems. We focus on cases that can be reasonably described by a two–region model. One is a standard tandem with plug (potential rise) assumed to exist throughout the anchor region. Here, we have passing electrons, and in the frame where the passing electrons see zero $E \times B$ drift we have a *positive* ω_C, which we found to be stable, *if* the anchor curvature-driven stability is sufficiently strong.

The second case is a tandem with a thermal barrier (potential depression) assumed to exist throughout the anchor and the final plugging potential to exist over essentially negligible length. Here we have passing ions, and a *negative* ω_C, which due to the sign change of the charge of the passing species is equivalent to our first case. That is, both of these cases have a shear mode tending to isolate to the anchor and so can be stabilized by sufficiently strong anchor curvature. But, both of these cases may still have a shear mode instability if the design of the tandem is too close to marginal stability based only on curvature drive. In this case there would in general be some significant mode amplitude in both the center cell and anchor, with the displacement in the anchor being somewhat larger, as per the discussion in sec. VI. A specific prediction can easily be generated by our numerical model for a given set of equilbrium numbers.

As a third example, the *negative* tandem is similar to our positive thermal barrier case, except for an additional constant negative potential, and so again we have passing

ions and negative ω_C, and again the prediction is stability to the shear mode if the anchor curvature stability is sufficiently strong.

We have seen that all three of the simplest two-region models of tandem mirrors are *stable* to the worst form of the shear mode, that where the mode tries to localize to the center cell. Indeed, since a rise(fall) in potential going from center cell to anchor means a positive(negative) ω_C, and to the extent that a rise(fall) in potential also means a greater electron(ion) passing density, then our model will always predict stability to the shear mode that goes unstable by localizing to the center cell. This prediction may possibly change when considering the variety of possible transient potential profiles occuring in real experiments. In any case, the rule of thumb developed here is easily checked against any possible (dominantly two–region) potential profile and its self–consistent passing density.

X. CONCLUSIONS

We have derived and numerically solved the equations for an electrostatic trapped particle mode that is driven by axial shear in the equilibrium $E \times B$ velocity, in the limit of the eikonal or high mode number approximation and for a restricted two region square well model of the equilibrium of a tandem mirror. The model includes competing effects of curvature and finite ion gyro radius. The results have considerably extended the results obtained by others,[3] particularly in the explanation of how the mode changes from its flute form, which is observed primarily in the low mode number limit and only in the zero curvature limit. The mode's principle characteristics are that it is more unstable for *larger* passing density, and that it may be unstable despite large anchor curvature by isolating to the center cell, without paying a line bending penalty since it is an electrostatic mode with no restrictions on $E_{\|}$. The physical mechanism of the mode in the nonflute regime is the differential $E \times B$ drifts between the fractional density n_p of trapped ions and the passing electrons. The usual charge separation mechanism for interchange instability will act to produce instability in the region with negative $\Delta\omega_E$ and to produce stability in the region

with positive $\Delta\omega_E$, thus tending to cause the mode to isolate to the former region. As a separate issue, there is also the possibility for increased stability(relative to zero shear) of the curvature driven trapped particle mode. This calculation was collisionless, but we have seen that our answer for the passing electron response, in the limit of 100% passing fraction, was identical to the strongly collisional answer,[5] as modified for our equilibrium.

Our model has two principal limitations. First, within the validity of the high mode number regime, our axial equilibrium model is too specialized and inappropriately allows arbitrary values of passing density, unrelated to other system parameters. A more realistic model would tie all parameters together with the appropriate equilibrium constraints. The value of our more loosely defined model is simply that it gave us the freedom to range over widely varying ranges of important variables, particularly the passing fraction, without worrying about the consistency issue. The physical insights gained from the results appear to be general and can now be applied to more realistic equilibria. One approach here would be to extend the number of axial square wells arbitrarily, with reasonable constraints established between passing fraction and potential differences between the various traps. The coupled equations approach, with root solving for ω, described in this paper, would directly carry over to such a model. For an axial equilbrium profile of any complexity, however, it may be more reasonable to go the full route of a completely continuous description of the orbits, which is most directly attacked with the initial value simulation technique.

The second limitation, the high mode number approximation, has four issues. One, the flute regime, $D >> 1$, may not be consistent with the high m limit. For example with $r/\rho_s = 10.$, $n_p = 1$, we have $D = 1.$ at $m = 10$, but with $n_p = 0.1$, $D = 1.$ at $m \approx 3 - 4$, so that in the latter case the flute regime can be reached only for $m \leq 3$. Two, finite gyro radius tends to stabilize the high mode numbers. Three, at low m, rotational modes driven by centrifugal force may be equally or more important than the velocity shear. Four, the low mode number regime may reveal different physical effects for the

shear mode, particularly in its nonflute form. For example, for a rigid $m = 1$ mode our differential $E \times B$ drift explanation of this paper would seem to be ineffectual, since, for this type of displacement the various species are simply drifting relative to a new center of rotation, and hence are drifting tangent to density contours and no charge separation is expected. But the flute limit has another physical explanation and may still occur for m = 1. We need the full radial solution to do more than make plausible arguments. A model that appears tractable to treat low mode numbers accurately is a radial gridded version of the present axial square well model. Root solving techniques may become too complicated, but initial value simulation techniques appear straightforward.

ACKNOWLEDGMENTS

The author would like to thank R. H. Cohen and W. M. Nevins for illuminating discussions, particularly with regard to the proper form for the electron Boltzmann response—early forms of this work were in error on this point. Work performed under the auspices of the U.S. Department of Energy by the Lawrence Livermore National Laboratory under contract number W-7405-ENG-48.

References

[1]X. S. Lee, P. J. Catto, and R. E. Aamodt, Phys. Fluids (25), 1491(1982)

[2]B. I. Cohen and R. Freis, private communication.

[3]H. L. Berk, M. N. Rosenbluth, H. V. Wong, T. M. Antonsen, D. E. Baldwin, Sov. J. Plasma Phys. vol(9) 108 (1983)

[4]J. A. Byers and R. H. Cohen, Phys. Fluids (28), 1591 (1985)

[5]W. M. Nevins, private communication.

Figure Captions

FIG. 1. Equilibrium axial profiles. Densities are shown as fractions of the total density, which is a constant in z. In (a) is shown the trapped ion density, in (b) the trapped electron densities, and in (c) the passing electron density. In (d) is shown the $E \times B$ drift frequency, in the frame where the passing density sees zero drift.

FIG. 2. Numerical solution of Eq. (16). In (a) growth rate vs mode number is plotted for the velocity shear mode with zero curvature and zero ion gyro radius, and for negative ω_C. The passing fraction, n_p, is a parameter. The straight line is the flute growth rate, given by $\gamma_f^2 = m^2\overline{(\Delta\omega_E)^2}$. In (b) the real frequency is plotted vs mode number for $n_p = 1.0$. Equilibrium values are $\delta = 0.25$, $r/\rho_s = 10.$, $\overline{\Omega_*}/m = \Delta\omega_E = 0.01\omega_{ci}$. Growth rate and frequency are dimensionless, normalized to $\Delta\omega_E$. In (c) the ratio of the displacement in the center cell to the displacement in the anchor is plotted vs mode number for the unstable range of mode numbers.

FIG. 3. Growth rate vs mode number in the presence of curvature. The parameter is the relative strength of the curvature driven flute stability, $\omega_{fc}^2/(\Delta\omega_E)^2$. In (a) for positive ω_C, complete stability occurs for $\omega_{fc}^2 \gtrsim 20(\Delta\omega_E)^2$. In (b) is shown the real frequency for one of the curves in (a). In (c), for negative ω_C, instability persists regardless of the magnitude of ω_{fc}^2. The center cell curvature driven growth rate is $\gamma_c = 0.01\omega_{ci} = \Delta\omega_E$. Other equilibrium values same as in Fig. 2, except for a change to $r/\rho_s = 5$, $\overline{\Omega_*}/m = 0.04\omega_{ci}$, which change has little effect on the unstable modes.

FIG. 4. Growth rate vs mode number in the presence of both curvature and finite ion gyro radius, with a_i/r a parameter, where $\omega_{*i}/\omega_{ci} = (a_i/r)^2$. Case (a) is for positive ω_C with curvature not quite sufficient to supply complete flute stability, $\omega_{fc}^2 = 125(\Delta\omega_E)^2$. Case (b) is for negative ω_C with curvature more than strong enough to supply flute stability, $\omega_{fc}^2 = 400(\Delta\omega_E)^2$. Equilibrium values are changed from the previous figures to $\overline{\Omega_*}/m = \Delta\omega_E = 0.001\omega_{ci}$, $r/\rho_s = 32.$, $\gamma_c = .003\omega_{ci} = 3\Delta\omega_E$, complete flute stability when $\omega_{fc}^2 \approx 200(\Delta\omega_E)^2$.

FIG. 5. Growth rate vs mode number with a_i/r as a parameter. Equilibrium parameters the same as Fig. 4b, except that the passing density is reduced from 1.0 to $n_p = 0.1$.

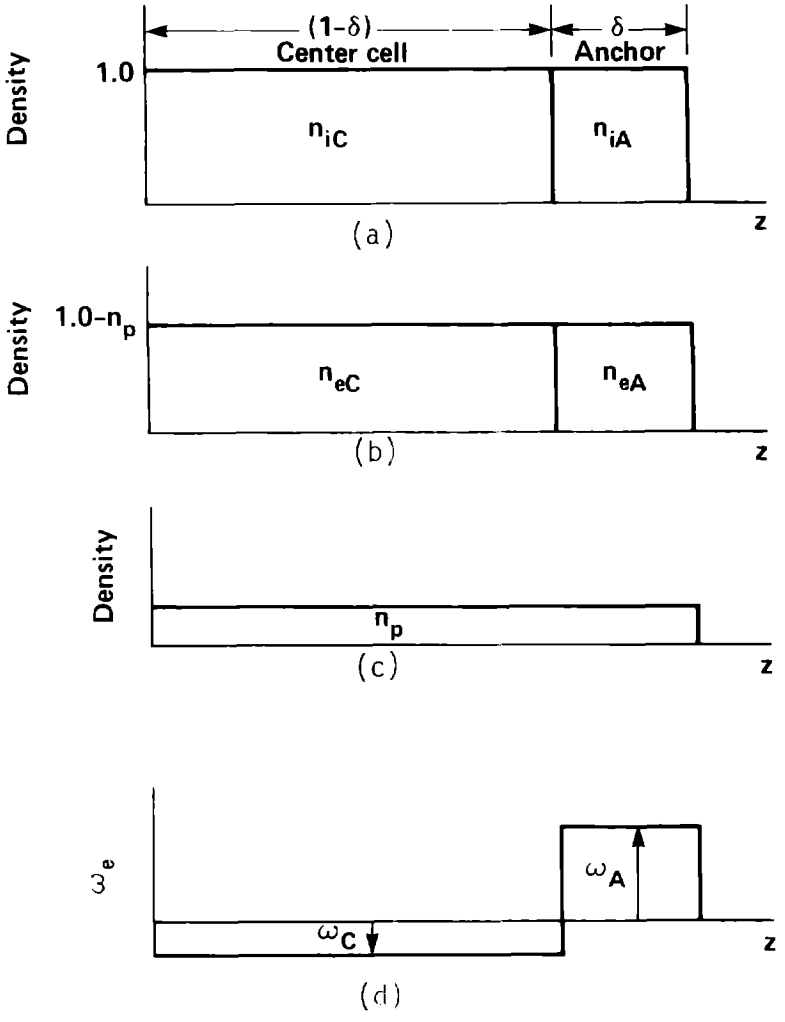
(1-δ)
Center cell
δ
Anchor
Density
1.0
n_{iC}
n_{iA}
z
(a)
Density
1.0-n_p
n_{eC}
n_{eA}
z
(b)
Density
n_p
z
(c)
ω_e
ω_A
ω_C
z
(d)

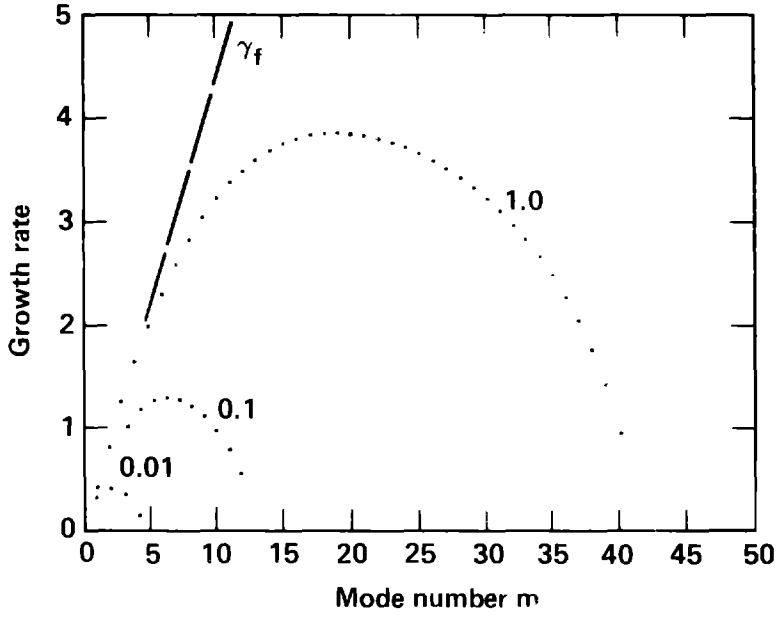
5
4
3
2
1
0
Growth rate
γ_f
1.0
0.1
0.01
0
5
10
15
20
25
30
35
40
45
50
Mode number m

Byers-Fig. 2b

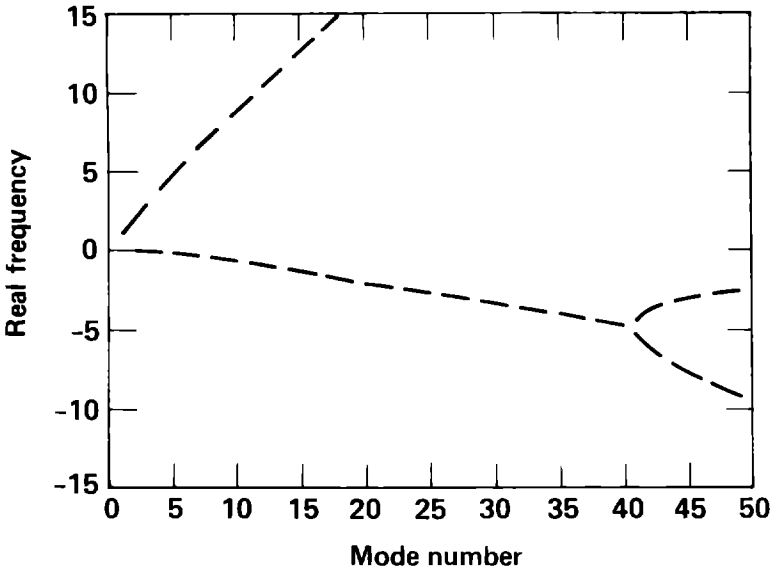
15
10
5
0
-5
-10
-15
Real frequency
0
5
10
15
20
25
30
35
40
45
50
Mode number

Byers-Fig. 2c

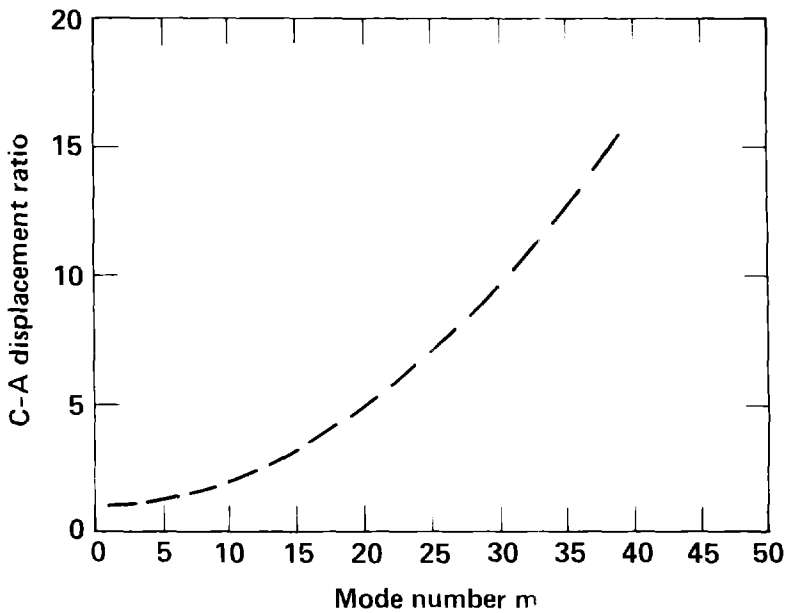
20
15
10
5
0
C-A displacement ratio
0
5
10
15
20
25
30
35
40
45
50
Mode number m

(a)

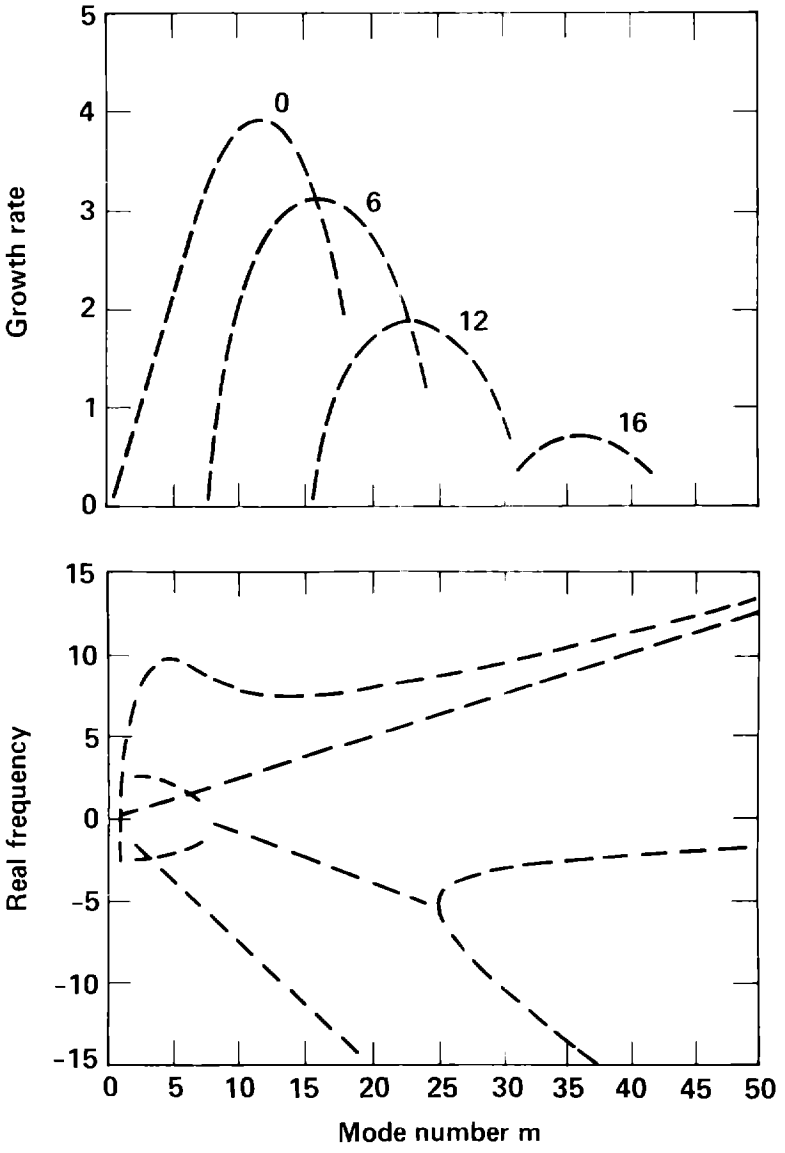
Growth rate
5
4
3
2
1
0
0
6
12
16
Real frequency
15
10
5
0
-5
-10
-15
0
5
10
15
20
25
30
35
40
45
50
Mode number m

(b)

Byers-Fig. 3c

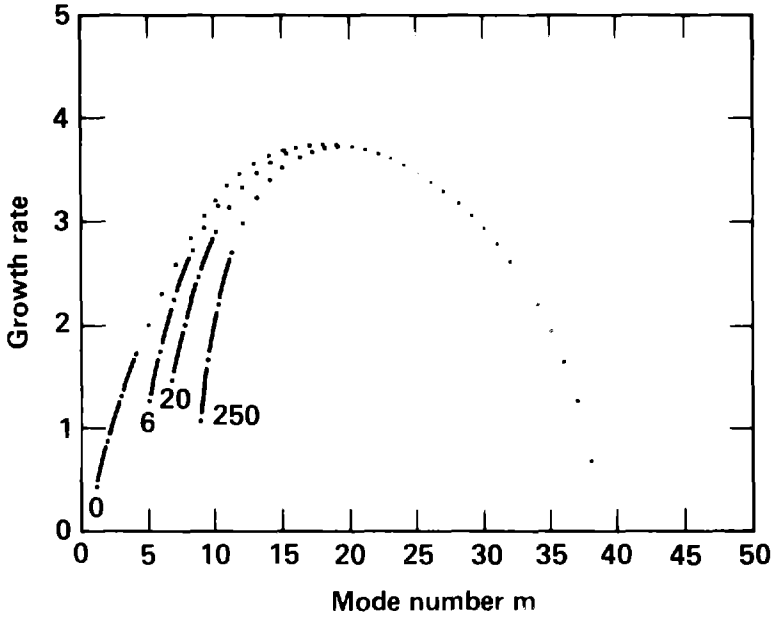
Growth rate
Mode number m
0
6
20
250
0
1
2
3
4
5
0
5
10
15
20
25
30
35
40
45
50

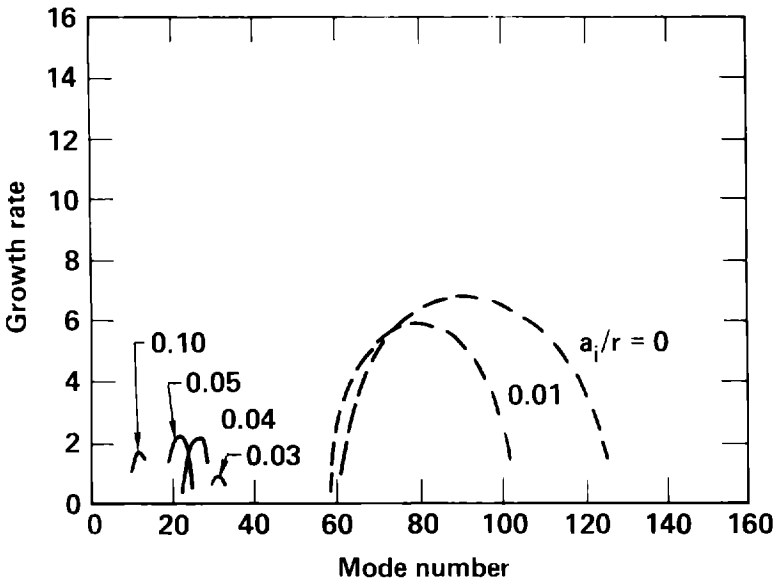
16
14
12
10
8
6
4
2
0
Growth rate
0.10
0.05
0.04
0.03
0.01
$a_i/r = 0$
0
20
40
60
80
100
120
140
160
Mode number

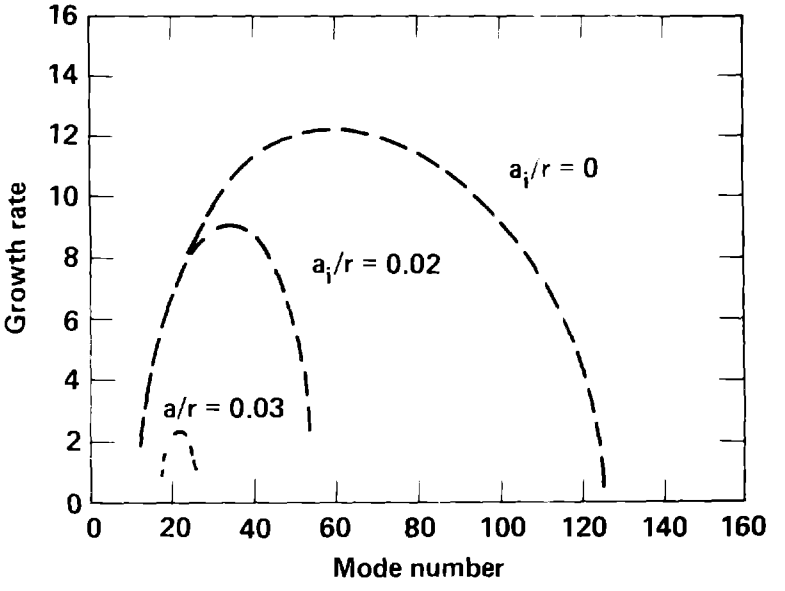
16
14
12
10
8
6
4
2
0
Growth rate
0
20
40
60
80
100
120
140
160
Mode number
$a_i/r = 0$
$a_i/r = 0.02$
$a/r = 0.03$

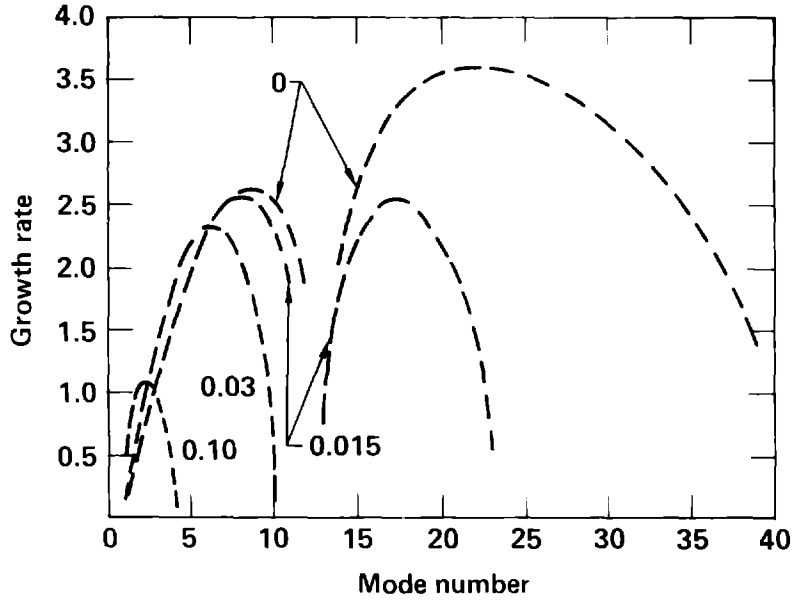
4.0
3.5
3.0
2.5
2.0
1.5
1.0
0.5
Growth rate
0
0.03
0.10
0.015
0
5
10
15
20
25
30
35
40
Mode number